HHS Public Access

Author manuscript

Nat Chem. Author manuscript; available in PMC 2022 May 01.

Published in final edited form as:

Nat Chem. 2022 January ; 14(1): 71–77. doi:10.1038/s41557-021-00802-2.

A biosynthetic pathway to aromatic amines that uses glycyl-tRNA as nitrogen donor

Page N. Daniels[1], **Hyunji Lee**[2], **Rebecca A. Splain**[2], **Chi P. Ting**[3], **Lingyang Zhu**[4], **Xiling Zhao**[2], **Bradley S. Moore**[5], **Wilfred A. van der Donk**[1,2,3,*]

[1]Department of Biochemistry, University of Illinois at Urbana-Champaign, Urbana, Illinois 61801, USA;

[2]Department of Chemistry and Howard Hughes Medical Institute, University of Illinois at Urbana-Champaign, Urbana, Illinois 61801, USA;

[3]Carl R. Woese Institute for Genomic Biology, University of Illinois at Urbana-Champaign, Urbana, Illinois 61801, USA;

[4]School of Chemical Sciences NMR Laboratory, University of Illinois at Urbana-Champaign, Urbana, Illinois 61801, USA;

[5]Scripps Institution of Oceanography, University of California, San Diego, La Jolla, CA 92037, USA.

Abstract

Aromatic amines in nature are typically installed with Glu or Gln as the nitrogen donor. Here we report a pathway that features glycyl-tRNA as the nitrogen donor. During the biosynthesis of pyrroloiminoquinone-type natural products such as ammosamide, peptide-aminoacyl tRNA ligases (PEARLs) append amino acids to the C-terminus of a ribosomally synthesized peptide. First, $AmmB_C^{Trp}$ adds Trp in a Trp-tRNA dependent reaction, and the flavoprotein $AmmC_1$ then carries out three hydroxylations of the indole ring of Trp. After oxidation to the corresponding *ortho*-hydroxy *para*-quinone, $AmmB_D^{Gly}$ attaches Gly to the indole ring in a Gly-tRNA dependent fashion. Subsequent decarboxylation and hydrolysis results in an amino-substituted indole. Similar transformations are catalyzed by orthologous enzymes from *Bacillus halodurans*. This pathway features three previously unknown biochemical processes using a ribosomally synthesized peptide as scaffold for non-ribosomal peptide extension and chemical modification to generate an amino acid derived natural product.

*To whom correspondence should be addressed: Wilfred A. van der Donk, 600 S. Mathews Avenue, Urbana, Illinois 61801, United States, vddonk@illinois.edu, phone: (217) 244-5360, fax: (217) 244-8533.

Author Contributions

P.N.D., H.L., R.A.S., C.P.T., and W.A.v.d.D. designed the study. P.N.D., H.L., R.A.S., C.P.T. and X.Z. performed all experiments. L.Z. acquired and interpreted the NMR data. B.S.M. provided reagents and helpful discussions; P.N.D. and W.A.v.d.D. wrote the manuscript.

Competing financial interests

The authors declare no competing interests.

Graphical Abstract

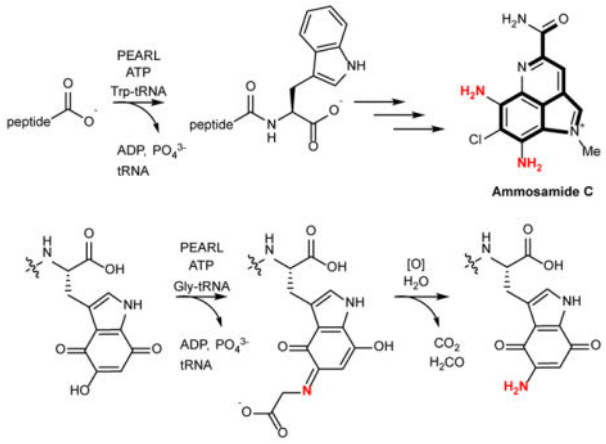

Pyrroloiminoquinones and related natural products are produced by a wide variety of organisms and have diverse bioactivities[1–5]. The ammosamides are a subset of pyrroloiminoquinones that are produced in various environments (Fig. 1a)[6–8]. This compound family displays antiproliferative activities against cancer cells with some members binding to myosin or inhibiting quinone reductase 2[6, 9–11]. The core structures of the ammosamides and lymphostin, another pyrroloiminoquinone, are derived from Trp[7, 12, 13]. Recent studies demonstrated that these compounds are biosynthesized via an unexpected posttranslational modification process in which a peptide aminoacyl-tRNA ligase (PEARL) adds Trp from tryptophanyl-tRNA to the C-terminus of a ribosomally produced scaffold peptide. This Trp is then converted to a pyrroloiminoquinone by an as-of-yet unknown pathway[14].

PEARLs display low sequence similarity to the N-terminal domain of LanB dehydratases involved in lanthipeptide biosynthesis (e.g. 11.2% identity/21.0% similarity between the PEARL TglB and the dehydratase NisB). The N-terminal domain of LanB uses glutamyl-tRNA to glutamylate the side chain hydroxyl groups of Ser and Thr residues in a substrate peptide followed by elimination of the Glu by the C-terminal domain to generate dehydroalanine and dehydrobutyrine, respectively[15–19]. PEARL enzymes have homology with the LanB glutamyl transferase domain but lack the elimination domain. They also use aminoacyl-tRNA as substrate but catalyze very different chemistry that first involves ATP-dependent phosphorylation of the C-terminus of a scaffold peptide, and then amide bond formation with the amino group of the aminoacyl-tRNA (Fig. 1b)[20]. This process is involved in the biosynthesis of a range of natural products by phylogenetically diverse bacteria, including the ammosamides and 3-thiaglutamate[7, 12, 14].

The ammosamide biosynthetic gene cluster (BGC) in *Streptomyces* sp. CNR-698 encodes four PEARL enzymes[7] (Fig. 2a), even though all carbon atoms found in ammosamide derive from Trp, and hence one PEARL that adds Trp appears sufficient. We demonstrate here a pathway by which PEARLs are utilized to introduce nitrogen atoms onto the indole of Trp, providing a general framework for pyrroloiminoquinone biosynthesis.

Our studies focused on the ammosamide BGC as well as a gene cluster in *Bacillus halodurans* C-125 that contains seven PEARL enzymes (Fig. 2a). We demonstrate that both BGCs encode a PEARL that adds Trp to a scaffold peptide. Next, a tetratricopeptide repeat (TPR) domain-containing flavoprotein oxidizes the indole of the tryptophan three times to generate a trihydroxyindole. This electron-rich structure is oxidized to the corresponding hydroxyquinone and converted to an aminoquinone via PEARL-catalyzed addition of Gly-tRNA, providing an unanticipated pathway to aromatic amines. These studies provide an unexpected use of PEARL enzymes for the amination of indoles.

Results and discussion

Analysis of the *amm* biosynthetic gene cluster

The *amm* BGC (Fig. 2a, Supplementary Table 1) contains a gene for a precursor peptide (*ammA*), four genes encoding PEARL enzymes (*ammB*$_{1–4}$), two genes encoding tetratricopeptide repeat (TPR) domain containing enzymes (*amm7/amm22)*, a glycine oxidase (*amm17*), several proteases (*amm12/19*), a chlorinase (*amm3*), and several proteins whose functions are not clear (Fig. 2a, Supplementary Table 1)[7]. A previous study showed that the precursor peptide is first trimmed back to a shorter peptide (termed AmmA*) that has homology with many other peptides that are encoded near PEARL enzymes in various BGCs (Supplementary Fig. 1 and 2). Removal of the seven C-terminal residues from AmmA reveals a C-terminal motif (APLALA) that is conserved in its homologs (Supplementary Fig. 2). AmmB$_2$ was shown to add a Trp from Trp-tRNA to the C-terminus of AmmA*[14]. The resulting peptide AmmA*-Trp was not a substrate for any of the four PEARL enzymes (Supplementary Fig. 3), which have low pair-wise sequence identities (Supplementary Table 2). Hence, the pathway by which the appended Trp is converted to a pyrroloiminoquinone remained unresolved.

We hypothesized that another posttranslational modification was needed before the next PEARL could act on the peptide. A strict order of PTMs has been reported for other RiPP biosynthetic pathways (*e.g.*[21–24]). Therefore, we interrogated the activity of the other proteins encoded in the *amm* biosynthetic gene cluster by co-expressing His$_6$-AmmA*-Trp with other enzymes in *Escherichia coli*. Upon purification of the peptides by immobilized metal affinity chromatography (IMAC), we found that co-expression with Amm7 resulted in a mass shift of +48 Da (peptide **A**) as observed by matrix-assisted laser desorption/ionization time-of-flight mass spectrometry (MALDI-TOF MS) (Fig. 2b). Smaller peaks of +16 and +32 Da were also observed suggesting possibly three hydroxylations. Subsequent treatment with trypsin and high-resolution mass spectrometry (HRMS) analysis revealed that the mass additions occurred on the C-terminal 8-mer fragment (Supplementary Fig. 4). Co-expression of AmmA*-Trp with Amm7 and each of the remaining PEARL enzymes (AmmB$_1$, AmmB$_3$, and AmmB$_4$) individually resulted only in a change in mass of peptide **A** for AmmB$_3$. A new product was observed that increased in mass by 11 Da (Fig. 2c, Supplementary Fig. 5). This mass increase was puzzling as it did not correspond to the anticipated addition of a proteinogenic amino acid. Poor yield did not allow characterization of the product, but the nature of the chemical transformations catalyzed by Amm7 and AmmB$_3$ were revealed by study of a related BGC in *B. halodurans* (Fig. 2a) as described in

the next sections. The orthologous enzymes from this BGC gave higher product yields in *E. coli* as well as intermediates that provided key additional insights.

Analysis of the *bha* biosynthetic gene cluster

The PEARL-containing *bha* gene cluster in *B. halodurans* exhibits several similarities to the ammosamide BGC (Fig. 2a, Supplementary Table 3). It contains genes for a precursor peptide (*bhaA*) with sequence similarity to AmmA*, seven instead of four PEARLs (*bhaB*$_{1–7}$), four TPR-domain containing enzymes with sequence homology to AmmC$_1$ (*bhaC*$_{1–4}$; Supplementary Fig. 6), a glycine oxidase (*bhaG*), TldD/E-like proteases (*bhaDE*)[25, 26], and several other proteins of unknown function that are not in the *amm* cluster (Fig. 2a, Supplementary Tables 1 & 3). Six of the seven PEARLs contain a typical RiPP recognition element (RRE)[27] that has been shown crystallographically to engage the substrate peptide for LanB enzymes[15]. The TldD/E-like proteins BhaD and BhaE are anticipated to proteolytically cleave the mature natural product from the scaffold peptide[25, 26]. Similar BGCs were found in a variety of organisms from several different bacterial phyla (for precursor peptides and accession numbers, see Supplementary Fig. 2a) suggesting a widespread occurrence. Attempts to activate the *bha* cluster in *B. halodurans* were unsuccessful (see Supplemental Information), prompting a combined biochemical and synthetic biology study of the enzymes involved.

BhaB$_1$ and BhaB$_7$ are aminoacyl-tRNA dependent amide bond forming enzymes

The BhaA peptide and its homologs (Fig. 2a and Supplementary Fig. 2) are highly acidic peptides (17 out of 39 residues are Asp or Glu). BhaA shares high sequence identity with the precursor peptide AmmA in the ammosamide BGC, but does not contain the seven amino acids at the C-terminus of AmmA (Supplementary Fig. 2a). Compared to its homologs and the truncated AmmA* peptide, BhaA lacks the C-terminal Ala of the APLALA motif (Fig. 2a, Supplementary Fig. 2). To determine which PEARL acts first in the *B. halodurans* pathway, each PEARL was co-expressed in *E. coli* with His$_6$-BhaA. Upon purification of the peptide by IMAC, MALDI-TOF MS analysis demonstrated that only co-expression with BhaB$_1$ changed the peptide mass, resulting in an increase of 71 Da (Fig. 3a,b). This increase is consistent with the condensation of an Ala residue. High resolution (HR) tandem mass spectrometry (MS/MS) analysis of the peptide compared to a synthetic standard confirmed that an Ala residue had been appended to the C-terminus of the peptide (Supplementary Fig. 7). The appendage of Ala adds to the known amino acids that are used by PEARLs, which to date included Cys and Trp[14]. In addition, the activity of BhaB$_1$ completes the APLALA motif that is present in BhaA homologs including AmmA* and compensates for the lack of an Ala at the C-terminus of BhaA.

We next investigated all remaining BhaB enzymes by co-expression in *E. coli* with the product of BhaB$_1$, BhaA-Ala, and discovered that BhaB$_7$ increases the peptide mass by 186 Da, consistent with the condensation of a Trp residue (Fig. 3b,c). MS/MS analysis of the peptide compared to a synthetic standard corroborated the appendage of Trp to the C-terminus of BhaA-Ala (Supplementary Fig. 8). Thus, unlike LanB dehydratases that to date have all been shown to transfer glutamate from glutamyl-tRNA to the side chain of Ser and Thr residues, the activities of PEARL enzymes are more diverse. We

propose nomenclature that helps to rapidly and concisely indicate the individual activities of these enzymes. We suggest that the term $LanB_A^{Glu}$ is used for canonical dehydratases that contain both glutamylation and elimination domains and that the term $LanB_B^{Glu}$ is used for the glutamylation component of "split LanB" enzymes that have the glutamylation and elimination activities in two separate polypeptides (e.g. thiopeptides and goadsporin)[21, 28]. We suggest the term $LanB_C^{Aaa}$ for PEARL enzymes that conjugate amino acids (Aaa) to the C-terminus of scaffold peptides. Thus, $AmmB_2$ would be $AmmB_C^{Trp}$, $BhaB_1$ would be $BhaB_C^{Ala}$, and $BhaB_7$ would be $BhaB_C^{Trp}$. We will use this terminology in the remainder of this study.

The transformation catalyzed by $BhaB_C^{Trp}$ is akin to the tryptophan condensation by $AmmB_C^{Trp}$ in the ammosamide biosynthetic pathway[14], thus providing an example of two PEARL enzymes that catalyze the same conjugation reaction. Sequence similarity analysis reveals that $AmmB_C^{Trp}$ and $BhaB_C^{Trp}$ are quite distinct from one another with only 20% sequence identity (Supplementary Table 2, Supplementary Fig. 9a). This difference in part may reflect the phylogeny of the producing organisms (Actinobacteria and Firmicutes) as is also observed for $LanB_A^{Glu}$ proteins[15, 29], and in part reflect different evolutionary paths given a number of insertions and deletions. Further studies will be required to characterize the molecular basis for amino acid specificity of PEARLs such that their activities may be predicted by bioinformatics.

In vitro incubation of purified His_6-$BhaB_C^{Ala}$ with BhaA, Ala, ATP, $tRNA^{Ala}$, and alanyl-tRNA synthetase (AlaRS) from *E. coli* resulted in the production of BhaA-Ala, just as was observed by co-expression. Omitting reagents from the assay demonstrated that the reaction is ATP-, tRNA-, and AlaRS-dependent (Supplementary Fig. 10). Similarly, *in vitro* reaction of purified $BhaB_C^{Trp}$ with BhaA-Ala, Trp, ATP, $tRNA^{Trp}$, and tryptophanyl-tRNA synthetase (TrpRS) from *E. coli* resulted in the production of BhaA-Ala-Trp (Supplementary Fig. 11).

$BhaC_1$ hydroxylates the indole of Trp

Similar to the observations with the *amm* BGC, no further modification was detected in *E. coli* upon co-expression of the $BhaB_C^{Ala}$ and $BhaB_C^{Trp}$ modified peptide (BhaA-Ala-Trp) with the remaining PEARLs in the BGC (Supplementary Fig. 12). The $AmmC_1$ homologs $BhaC_1$, -C_2, -C_3, -C_4, are all TPR-domain containing proteins, but analyses using various bioinformatics tools (Pfam, BLAST, HHpred, Phyre2 modeling) do not provide any additional hints regarding function or cofactor use. TPR-domains contain a series of consensus residues that generate alpha-solenoid structures that usually mediate protein-protein interactions[30–34]. Upon co-expression with His_6-BhaA-Ala-Trp, of the four BhaC proteins, only $BhaC_1$ led to a change in the mass of the peptide, increasing it by 48 Da (Fig. 3d,e), consistent with the observations with $AmmC_1$ (Fig. 2b). To evaluate the site of putative oxidation, the peptide product was treated with LysC endoproteinase and the resulting C-terminal 8-mer peptide was subjected to MS/MS analysis, demonstrating

that the +48 Da modification was to the C-terminal Trp residue (Supplementary Fig. 13). The enzymatic product readily oxidized resulting in a 2 Da mass loss and alteration of the spectral properties of the peptide, which turned pink in color (peptide **B**, Supplementary Fig. 14 and 15). NMR and MS data on peptide **B** after protease treatment are consistent with conversion of the indole of Trp to a 5-hydroxyquinone structure (Fig. 3g; Supplementary Fig. 16 and 17) and also demonstrates the high reactivity of **B** (see Supplementary Information).

We next expressed His_6-$BhaC_1$in *E. coli* and purified the enzyme by IMAC. Mass spectrometric analysis of the purified protein revealed the presence of flavin mononucleotide (FMN) (Supplementary Fig. 18), consistent with the yellow color of the enzyme. $BhaC_1$ was not predicted bioinformatically to be a flavoprotein and no obvious flavin binding signatures could be detected in its sequence. *In vitro* His_6-$BhaC_1$ also oxidized BhaA-Ala-Trp three times (Supplementary Fig. 19), and intermediates with one (+16 Da) and two hydroxylations (+32 Da) were also observed. These intermediates could not be separated, preventing investigation of the order of the modifications, but the observation of +16 and +32 Da products further supports the assignment of the +48 Da product resulting from three hydroxylations. The oxidation catalyzed by $BhaC_1$ (and $AmmC_1$ as discussed above) is an unusual example of post-translational trihydroxylation of tryptophan by a single enzyme[35–40].

$BhaB_5$ adds glycine from Gly-tRNA to the indole of Trp

After observing the hydroxylation of the Trp, we revisited the PEARLs within the cluster to assess whether any of the remaining five BhaB enzymes would act on this modified peptide as was observed with the $AmmC_1$-oxidized AmmA*-Trp and $AmmB_3$ (Fig. 2c). Upon co-expression of BhaA-Ala-Trp, $BhaC_1$ and either $BhaB_2$, -B_3, -B_4, -B_5, or -B_6, the only change in the mass of the BhaA peptide was observed with $BhaB_5$ (Fig. 3f). MALDI-TOF MS analysis of the products after IMAC purification showed three products (ions associated with compounds **D**, **E**, and **F**, Fig. 3f,g). Notably, compound **E** is the equivalent product that was observed upon co-expressing AmmA*-Trp with $AmmC_1$ and $AmmB_3$ (+11 Da from peptide **A**, Fig. 2c). A minor product (corresponding to peak **D**) corresponded to an increased mass of +55 Da from the trihydroxylated Trp-containing peptide (or +57 Da from the quinone-containing pink peptide **B**). Based on the presumption that PEARLs append amino acids to scaffold peptides, the mass shift was consistent with the condensation of Gly to the C-terminus of the peptide. The product peptide was digested with endoproteinase LysC and subjected to HR-MS, which provided data consistent with the addition of Gly (Supplementary Fig. 20). MS/MS analysis corroborated the appendage of a +57 Da moiety to the C-terminal Trp, but the expected y ion corresponding to a glycine fragment by amide bond fragmentation was not detected (Supplementary Fig. 21). The amounts of product **D** were very small, but scale-up allowed isolation of sufficient material to record an HMBC spectrum, which surprisingly revealed that the appended Gly was attached to C5 of the oxidized indole of the modified Trp residue (Fig. 3g) as indicated by several diagnostic cross peaks (Supplementary Fig. 22).

This transformation at first glance appears very different from the chemistry catalyzed by other PEARLs, which predicted the Gly to be attached to the C-terminal carboxylate. However, as noted above, *in vitro* the initial trihydroxylated Trp is readily oxidized to the corresponding *ortho*-hydroxy-*para*-quinone (**B**, Fig. 3g). By the concept of vinylogy[41], the hydroxyl group at C5 in this intermediate is expected to have similar reactivity as a carboxylic acid. Thus, based on the mechanism previously determined for the PEARL TglB[20], we propose that $BhaB_5$ phosphorylates the hydroxyl group at position 5 in the *ortho*-hydroxy quinone **B** to generate intermediate **pB** (Fig. 3g) followed by attack of the amino group of glycyl-$tRNA^{Gly}$ onto C5 to form a tetrahedral intermediate and elimination of phosphate to yield intermediate **C**. Subsequent hydrolysis of the tRNA, as previously demonstrated for TglB[14], would give intermediate **D**. The MS and NMR data (Supplementary Fig. 20–22) are fully consistent with this assignment and are suggestive of the formation of tautomer **D'** (Fig. 3g). It is possible that the on-pathway intermediate is **D** and that a small amount of peptide dissociates from the enzyme and tautomerizes to **D'**, thereby allowing detection and isolation of the intermediate by preventing decarboxylation. Because $BhaB_5$ does not add an amino acid to the C-terminus of a peptide, we propose that enzymes that catalyze similar chemistry will be termed $LanB_D^{Aaa}$, with $BhaB_5$ named $BhaB_D^{Gly}$.

Closer analysis of the other two products formed in the reaction of $BhaB_D^{Gly}$ by MALDI-TOF MS (peaks **E/E'** and **F**, Fig. 3f) provides additional support that the addition of Gly to C5 on the indole of Trp is on pathway to pyrroloiminoquinone formation. At first glance, the mass spectrum suggests that the reaction did not go to completion and that most of the oxidized BhaA-Ala-Trp (**B**) was unreacted. However, treatment with endoproteinase AspN to shorten the peptide and subsequent high-resolution electrospray ionization (ESI) MS analysis demonstrated that the mass of the peptide had decreased by 1 Da compared to peptide **B** (Supplementary Fig. 23). The most likely explanation is conversion of the *ortho*-hydroxy-*para*-quinone to an *ortho*-amino-*para*-quinone (**F**, Fig. 3g). *In vitro* experiments discussed below support this assignment.

The third product of the $BhaB_D^{Gly}$ reaction (peak **E/E'**, Fig. 3g) is the equivalent product observed originally in the $AmmB_3$ reaction (Fig. 2c). The peptide displays an ion with a mass that is increased by 11 Da from the hydroxyquinone and decreased by 44 Da from the Gly adduct **D**/**D'** consistent with decarboxylation of intermediate **D** to compound **E** or its tautomer **E'**. We propose that product **F** is formed upon oxidation of the electron rich indole of peptide **E**, which would facilitate hydrolysis of the imine to the amine (Fig. 3g). This oxidation is not seen to the same extent when AmmA*-Trp was co-expressed with $AmmC_1$ and $AmmB_3$ ($AmmB_D^{Gly}$) in *E. coli* (Fig. 2c), nor is it observed to the same extent *in vitro* with the Bha enzymes (see below). Thus, we propose that this step is normally catalyzed by one of the redox enzymes in the *amm* and *bha* BGCs (Supplementary Tables 1 and 2) and that the oxidation observed in Fig. 3f is due to serendipitous oxidation in *E. coli*. Indeed, the extent of oxidation also varies in different *E. coli* expression strains (e.g. Supplementary Fig. 25). The oxidation and hydrolysis of intermediate **E/E'** prevented NMR characterization

as the intermediate was converted to **F** during the extended time required (Supplementary Fig. 24). Intermediate **F** proved very reactive like quinone **B** (Supplementary Figs. 16 and 17), and decomposed non-enzymatically into multiple products that show fragment ions in the MS-MS that are consistent with cyclization and dimerization products but that we were unable to fully assign.

To provide further support for the mechanism in Fig. 3g and the structural assignments, the $BhaB_5$ reaction was reconstituted *in vitro* confirming the requirement of glycyl-tRNA and ATP (Supplementary Fig. 26). Use of [^{15}N,$^{13}C_2$, $^{2}H_2$]-Gly resulted in mass shifts for peptides **D/D'**, **E/E'**, and **F** consistent with their assignments (Supplementary Figs. 27–30).

One aspect of the proposed model requires further discussion. The products of the $AmmC_1$ and $BhaC_1$ enzymes formed in *E. coli* are colorless and contain Trp with a trihydroxyindole. Only upon purification and exposure to air in the absence of reducing agents do these peptides oxidize and take on a pink color. The question thus arises how $AmmB_3$ and $BhaB_5$ can add Gly in *E. coli* as observed (Fig. 2c and 3f). We propose that the electron rich trihydroxyindole is oxidized to the quinone in cells but that the reducing environment readily reverses this oxidation. But when $AmmB_3$ or $BhaB_5$ are co-expressed, they convert the small amount of hydroxyquinone-containing peptides to the Gly adduct. We suspect that the oxidation of **A** to **B** in the physiological pathway may be carried out by one of several redox enzymes in the BGCs (Supplementary Tables 1 and 3). This hypothesis also suggests that the originally formed product **A** is not a substrate for $AmmB_3$ or $BhaB_5$. This prediction was confirmed for $BhaB_5$, which did not react with **A** under anaerobic conditions (Supplementary Fig. 31). Because $AmmB_3$ does not accumulate intermediate **D**/**D'** observed with $BhaB_5$, we could not confirm that the attachment site of Gly is also C5. An alternative possibility is C7 since the hydroxyquinone **B** could exist in a tautomeric form where phosphorylation could occur at O7. Such putative alternative regiochemistry could explain why the imine product appears to accumulate more in *E. coli* for AmmA than BhaA (Figures 2c and 3f).

An alternative route to aromatic amines

The current study, and the occurrence of similar BGCs in various bacteria, reveals an unexpected route by which nature accesses aromatic amines in a range of different phyla. Previously characterized pathways to these common structural motifs use the canonical amino group donors Glu and Gln during amino transfer events (Fig. 4). In these pathways, the amino group is introduced prior to aromatization. In an unusual case in roseoflavin biosynthesis[42–45], aromatic amine biosynthesis takes place on a substrate that is already aromatic, but the nitrogen donor is still Glu (Fig. 4). An alternative route reported in this work introduces amino groups starting from a phenolic precursor and using glycine from glycyl-tRNA as the amino group donor.

Our findings allow a proposed pathway to the pyrroloiminoquinone scaffold of the ammosamides. The current study demonstrates the conversion of Trp to an aminoquinone by $AmmC_1$ and $AmmB_3$. Two more amino groups would need to be introduced to form the skeleton of the ammosamides (Fig. 1a), which can be achieved by two more cycles of addition of glycyl-tRNA by the two remaining AmmB proteins ($AmmB_1$ and $AmmB_4$).

Supplementary Fig. 32 presents a pathway to ammosamide C using a combination of the proteins encoded in the *amm* BGC. Thus, the current study provides insights into how a Trp appended at the C-terminus of a ribosomal peptide can be transformed into a pyrroloiminoquinone using post-translational modifications.

This work also demonstrates an interesting difference between the $AmmB_C^{Trp}$ and $AmmB_D^{Gly}$ enzymes and their BhaB orthologs compared to the $LanB_A^{Glu}$ and $LanB_B^{Glu}$ dehydratases. The latter enzymes have been demonstrated to be selective for the $tRNA^{Glu}$ sequence of their producing organisms in both lanthipeptide and thiopeptide biosynthesis. For instance, glutamyl-tRNA dependent dehydratases involved in microbisporicin and thiomuracin biosynthesis showed poor activity with glutamyl-tRNA from *E. coli* and were fully active only with tRNA from Actinobacteria[21, 46]. In contrast, $AmmB_C^{Trp}$ and $AmmB_D^{Gly}$ from *Streptomyces* sp. CNR-698 and $BhaB_C^{Trp}$ and $BhaB_D^{Gly}$ from *Bacillus halodurans* C-125 were active in *E. coli* and therefore do not appear to require tRNA sequences from their producing organism (see Supplementary Fig. 33 for a comparison of tRNA sequences). Although more examples will need to be investigated to determine if this conclusion is general, from an evolutionary perspective a relaxed specificity with respect to the tRNA sequence would be beneficial for evolving new activities and selectivities, which may explain the diversity of aminoacyl-tRNAs utilized by $LanB_{C/D}$ enzymes.

Methods

For protein expression, purification, and in vitro assays, see the Supplemental Information.

In vitro transcription of tRNAs

Primers for *E. coli* $tRNA^{Ala}$, $tRNA^{Trp}$, and $tRNA^{Gly}$ were designed according to a previously described method[47]. The tRNA dsDNA templates were generated from two overlapping synthetic deoxyoligonucleotides (Supplementary Table 4). To prepare the dsDNA template for in vitro transcription, 5′ overhangs were filled in using the following conditions: NEB Buffer 2 (1×), primers (4 μM each), dNTP (100 μM each), and DNA polymerase I large (Klenow) fragment (1 U μg^{-1} DNA) in a final volume of 50 μL. The reaction was incubated at 25 °C for 15 min, quenched with EDTA (10 mM) at 75 °C for 25 min, and dsDNA templates were precipitated with cold EtOH overnight. In vitro transcription was performed using a previously described method[48]. The transcribed tRNA was then purified by acidic phenol extraction using a previously described method[49].

Co-expression experiments and peptide purification

For plasmid preparation, see the Supplementary Information. *E. coli* BL21 (DE3) cells (New England Biolabs) expressing N-terminal His_6-tagged BhaA variants (BhaA, BhaA-Ala, BhaA-Ala-Trp) were grown with the following antibiotic markers. Cells containing *His_6-BhaA-pET28b* (Fig. 3a) or *His_6-BhaA-Ala-pET28b* were grown with 50 μg/mL kanamycin. Cells containing *His_6-BhaA-Ala-Trp-pETDuet-1* were grown with 100 μg/mL ampicillin. For co-expression systems of *bha*, the $BhaB_1$ and $BhaB_7$-modified peptides were obtained by using pRSFDuet-1 with the peptide (His_6-BhaA or His_6-BhaA-Ala) encoded in multiple

cloning site 1 (MCS1) and the PEARL enzyme encoded in MCS2 (Fig. 3b–c). These celles were grown with 50 μg/mL kanamycin. For the co-expression of BhaA-Ala-Trp with $BhaC_1$ we observed that the enzyme did not fully process the substrate when the peptide was expressed from a high copy number plasmid like pETDuet-1 (~40 copies) or pRSFDuet-1 with the enzyme inserted in (MCS2) of the same vector. Therefore, new constructs were redesigned with the peptide BhaA-Ala-Trp expressed from pACYCDuet, which has a lower copy number (10–12 copies), and BhaC1 from pET28b (copy number ~40). This change results in a peptide that has a slightly different N-terminal sequence compared to BhaA-Ala-Trp formed by $BhaB_1$ and $BhaB_7$ expressed from pRSFDuet-1 (pRSFDuet-1, GSSHHHHHHSSGLVPRGSH- Fig. 3c vs pACYCDuet, GSSHHHHHHS- Fig. 3d). Most importantly, this switch resulted in full oxidation of BhaA-Ala-Trp by $BhaC_1$. Cells containing *His_6-BhaA-Ala-Trp-pACYCDuet-1* were grown with 25 μg/mL chloramphenicol (Fig. 3d–f).

All cells were grown in terrific broth (TB) media (for 1 L total: 20 g bacto tryptone, 24 g yeast extract, 2.3 g KH_2PO_4, 12.5 g K_2HPO_4, and 0.4% glycerol). Cultures were grown with shaking at 37 °C to an OD_{600} = 0.5–0.7, upon which 0.4 mM IPTG was added to induce peptide expression. Cells were harvested after 18 h and resuspended in lysis buffer (50 mM HEPES, 100 mM NaCl, pH 7.5), then lysed by sonication.

Peptides were purified by IMAC. The lysate was clarified by centrifugation at 50,000 relative centrifugal force (rcf) and applied to 3 mL of Ni-NTA-resin gravity flow column (Clonetec). The immobilized peptide was washed with 5 column volumes (CV) of wash buffer (50 mM HEPES, 100 mM NaCl, pH 7.5, 50 mM imidazole), and eluted with 100% elution buffer (50 mM HEPES, 100 mM NaCl, pH 7.5, 500 mM imidazole). The elution fraction was concentrated using a 3 kDa MWCO Amicon spin filter and washed with 10–20 CV of deionized water to remove imidazole, and the peptide solution was lyophilized.

E. coli strains BW25113 ΔtldDE:*kan* (DE3) or BL21 (DE3) (New England Biolabs) were transformed with the plasmid systems for peptide expression, expressing N-terminal His_6-tagged BhaA and variants (BhaA, BhaA-Ala, BhaA-Ala-Trp, BhaA-Ala-Trp*, BhaA-Ala-Trp*Gly). The cultures were grown with 50 μg/mL kanamycin for *E. coli* BL21 expressing BhaA and Bha-Ala and BhaA-Ala-Trp in pET28b or pRSFDuet-1, 25 μg/mL kanamycin and 12.5 μg/mL chloramphenicol for *E. coli* BW25113 ΔtldDE:*kan* (DE3) expressing BhaA-Ala-Trp, 16.6 μg/mL kanamycin, 8.3 μg/mL chloramphenicol, and 33.3 μg/mL carbenicillin for *E. coli* BW25113 ΔtldDE:*kan* (DE3) expressing BhaA-Ala-Trp* and BhaA-Ala-Trp*Gly in pACYCDuet-1, 12.5 μg/mL chloramphenicol for *E. coli* BL21(DE3) expressing BhaA-Ala-Trp, and 12.5 μg/mL chloramphenicol and 50 μg/mL carbenicillin for *E. coli* BL21(DE3) expressing BhaA-Ala-Trp* and BhaA-Ala-Trp*Gly in pACYCDuet-1 in TB media (for 1 L total: 20 g bacto tryptone, 24 g yeast extract, 2.3 g KH_2PO_4, 12.5 g K_2HPO_4, and 0.4% glycerol). Cultures were grown with shaking at 37 °C to an OD_{600} = 0.5–0.7, upon which 0.4 mM isopropyl β-D-1-thiogalactopyranoside (IPTG) was added to induce peptide and protein expression. Cells were harvested after 18 h and resuspended in lysis buffer, then lysed by sonication. Peptides were purified by IMAC as described above.

For expression of *amm* peptides, a similar procedure was followed except *E. coli* BL21 (DE3) cells (New England Biolabs) expressing N-terminal His_6-tagged AmmA variants (AmmA* or AmmA*-Trp) from *His_6-AmmA-pACYCDuet-1* were grown with 33 μg/mL chloramphenicol in LB media (for 1 L total: 10 g bacto tryptone, 5 g yeast extract and 10 g sodium chloride). Modified peptides were obtained by co-expression using pET28a-ammC$_1$ and pACYCDuet-1 plasmid containing *ammA** in MCS1 and *ammB3* in MCS2. *E. coli* BL21 (DE3) cells expressing N-terminal His_6-tagged modified AmmA* variants were grown with 17 μg/mL chloramphenicol and 25 μg/mL kanamycin in LB media. Cultures were grown with shaking at 37 °C to an OD600 = 0.5–0.7, upon which 0.4 mM IPTG was added to induce peptide and protein expression. Cells were harvested after 18 h and resuspended in lysis buffer, then lysed by sonication. Peptides were purified by IMAC as described above.

Data availability

The raw data associated with the spectra in Figures 2 and 3, and Supplementary Figures 3–5, 7, 8, and 10–15, 17–21, and 23–31 were deposited at Mendeley (van der Donk, Wilfred (2021), “PEARL 2021”, Mendeley Data, V1, doi: 10.17632/mk3ttnbt5t.1).

Supplementary Material

Refer to Web version on PubMed Central for supplementary material.

Acknowledgments

This work was supported by the National Institutes of Health (R37 GM058822 to W.v.d.D., T32 GM070421 to P.N.D, F32 GM105297 to R.S., F32 GM129944 to C.P.T., and R01 GM085770 to B.S.M.). We thank Dr. Michael A. Funk and Kwo-Kwang Abraham Wang for initial attempts to activate the *bha* cluster and Deborah A. Berthold for help in purifying GlyQS.

References

1. Lin S et al. Another look at pyrroloiminoquinone alkaloids-perspectives on their therapeutic potential from known structures and semisynthetic analogues. Marine Drugs 15, 98 (2017).
2. Peters S & Spiteller P Sanguinones A and B, blue pyrroloquinoline alkaloids from the fruiting bodies of the mushroom Mycena sanguinolenta. J. Nat. Prod 70, 1274–1277 (2007). [PubMed: 17658856]
3. Legentil L, Benel L, Bertrand V, Lesur B & Delfourne E Synthesis and antitumor characterization of pyrazolic analogues of the marine pyrroloquinoline alkaloids: wakayin and tsitsikammamines. J. Med. Chem 49, 2979–2988 (2006). [PubMed: 16686539]
4. Hu JF, Fan H, Xiong J & Wu SB Discorhabdins and pyrroloiminoquinone-related alkaloids. Chem. Rev 111, 5465–5491 (2011). [PubMed: 21688850]
5. Chen QB, Xin XL, Yang Y, Lee SS & Aisa HA Highly conjugated norditerpenoid and pyrroloquinoline alkaloids with potent PTP1B iinhibitory activity from *Nigella glandulifera*. J. Nat. Prod 77, 807–812 (2014). [PubMed: 24593120]
6. Hughes CC, MacMillan JB, Gaudencio SP, Jensen PR & Fenical W The ammosamides: structures of cell cycle modulators from a marine-derived *Streptomyces* species. Angew. Chem. Int. Ed 48, 725–727 (2009).
7. Jordan PA & Moore BS Biosynthetic pathway connects cryptic ribosomally synthesized posttranslationally modified peptide genes with pyrroloquinoline alkaloids. Cell Chem. Biol 23, 1504–1514 (2016). [PubMed: 27866908]

8. Reimer D & Hughes CC Thiol-based probe for electrophilic natural products reveals that most of the ammosamides are artifacts. J. Nat. Prod 80, 126–133 (2017). [PubMed: 28055208]
9. Reddy PV, Banerjee B & Cushman M Efficient total synthesis of ammosamide B. Org. Lett 12, 3112–3114 (2010). [PubMed: 20515072]
10. Hughes CC, MacMillan JB, Gaudencio SP, Fenical W & La Clair JJ Ammosamides A and B target myosin. Angew. Chem. Int. Ed. Engl 48, 728–732 (2009). [PubMed: 19097126]
11. Luo J et al. Discovery of ammosesters by mining the *Streptomyces uncialis* DCA2648 genome revealing new insight into ammosamide biosynthesis. J. Ind. Microbiol. Biotechnol, 10.1093/jimb/kuab1027 (2021).
12. Miyanaga A et al. Discovery and assembly-line biosynthesis of the lymphostin pyrroloquinoline alkaloid family of mTOR inhibitors in *Salinispora* bacteria. J. Am. Chem. Soc 133, 13311–13313 (2011). [PubMed: 21815669]
13. Colosimo DA & MacMillan JB Ammosamides unveil novel biosynthetic machinery. Cell Chem. Biol 23, 1444–1446 (2016). [PubMed: 28009976]
14. Ting CP et al. Use of a scaffold peptide in the biosynthesis of amino acid-derived natural products. Science 365, 280–284 (2019). [PubMed: 31320540]
15. Ortega MA et al. Structure and mechanism of the tRNA-dependent lantibiotic dehydratase NisB. Nature 517, 509–512 (2015). [PubMed: 25363770]
16. Garg N, Salazar-Ocampo LM & van der Donk WA In vitro activity of the nisin dehydratase NisB. Proc. Natl. Acad. Sci. U. S. A 110, 7258–7263 (2013). [PubMed: 23589847]
17. Repka LM, Chekan JR, Nair SK & van der Donk WA Mechanistic understanding of lanthipeptide biosynthetic enzymes. Chem. Rev 117, 5457–5520 (2017). [PubMed: 28135077]
18. Repka LM, Hetrick KJ, Chee SH & van der Donk WA Characterization of leader peptide binding during catalysis by the nisin dehydratase NisB. J. Am. Chem. Soc 140, 4200–4203 (2018). [PubMed: 29537838]
19. Bothwell IR et al. Characterization of glutamyl-tRNA-dependent dehydratases using nonreactive substrate mimics. Proc. Natl. Acad. Sci. U. S. A 116, 17245–17250 (2019). [PubMed: 31409709]
20. Zhang Z & van der Donk WA Nonribosomal peptide extension by a peptide amino-acyl tRNA ligase. J. Am. Chem. Soc 141, 19625–19633 (2019). [PubMed: 31751505]
21. Hudson GA, Zhang Z, Tietz JI, Mitchell DA & van der Donk WA In vitro biosynthesis of the core scaffold of the thiopeptide thiomuracin. J. Am. Chem. Soc 137, 16012–16015 (2015). [PubMed: 26675417]
22. Bewley KD et al. Capture of micrococcin biosynthetic intermediates reveals C-terminal processing as an obligatory step for in vivo maturation. Proc. Natl. Acad. Sci. USA 113, 12450–12455 (2016). [PubMed: 27791142]
23. Sikandar A, Franz L, Melse O, Antes I & Koehnke J Thiazoline-specific amidohydrolase PurAH Is the gatekeeper of bottromycin biosynthesis. J. Am. Chem. Soc 141, 9748–9752 (2019). [PubMed: 31192589]
24. Severinov K & Nair SK Microcin C: biosynthesis and mechanisms of bacterial resistance. Future Microbiol 7, 281–289 (2012). [PubMed: 22324995]
25. Allali N, Afif H, Couturier M & Van Melderen L The highly conserved TldD and TldE proteins of *Escherichia coli* are involved in microcin B17 processing and in CcdA degradation. J. Bacteriol 184, 3224–3231 (2002). [PubMed: 12029038]
26. Ghilarov D et al. The origins of specificity in the microcin-processing protease TldD/E. Structure 25, 1549–1561.e1545 (2017). [PubMed: 28943336]
27. Burkhart BJ, Hudson GA, Dunbar KL & Mitchell DA A prevalent peptide-binding domain guides ribosomal natural product biosynthesis. Nat. Chem. Biol 11, 564–570 (2015). [PubMed: 26167873]
28. Ozaki T et al. Insights into the biosynthesis of dehydroalanines in goadsporin. ChemBioChem 17, 218–223 (2016). [PubMed: 26630235]
29. Zhang Q, Yu Y, Velásquez JE & van der Donk WA Evolution of lanthipeptide synthetases. Proc. Natl. Acad. Sci. U. S. A 109, 18361–18366 (2012). [PubMed: 23071302]

30. Zhang M et al. The non-canonical tetratricopeptide repeat (TPR) domain of fluorescent (FLU) mediates complex formation with glutamyl-tRNA reductase. J. Biol. Chem 290, 17559–17565 (2015). [PubMed: 26037924]
31. Perez-Riba A & Itzhaki LS The tetratricopeptide-repeat motif is a versatile platform that enables diverse modes of molecular recognition. Curr. Opin. Struct. Biol 54, 43–49 (2019). [PubMed: 30708253]
32. Pallen MJ, Francis MS & Futterer K Tetratricopeptide-like repeats in type-III-secretion chaperones and regulators. FEMS Microbiol. Lett 223, 53–60 (2003). [PubMed: 12799000]
33. Das AK, Cohen PW & Barford D The structure of the tetratricopeptide repeats of protein phosphatase 5: implications for TPR-mediated protein-protein interactions. EMBO J 17, 1192–1199 (1998). [PubMed: 9482716]
34. Lamb JR, Tugendreich S & Hieter P Tetratrico peptide repeat interactions: to TPR or not to TPR? Trends Biochem. Sci 20, 257–259 (1995). [PubMed: 7667876]
35. Fitzpatrick PF Structural insights into the regulation of aromatic amino acid hydroxylation. Curr. Opin. Struct. Biol 35, 1–6 (2015). [PubMed: 26241318]
36. Fitzpatrick PF Mechanism of aromatic amino acid hydroxylation. Biochemistry 42, 14083–14091 (2003). [PubMed: 14640675]
37. Perdivara I, Deterding LJ, Przybylski M & Tomer KB Mass spectrometric identification of oxidative modifications of tryptophan residues in proteins: chemical artifact or post-translational modification? J. Am. Soc. Mass Spectrom 21, 1114–1117 (2010). [PubMed: 20219394]
38. Basran J et al. The mechanism of formation of N-formylkynurenine by heme dioxygenases. J. Am. Chem. Soc 133, 16251–16257 (2011). [PubMed: 21892828]
39. Hirose Y et al. Involvement of common intermediate 3-hydroxy-L-kynurenine in chromophore biosynthesis of quinomycin family antibiotics. J. Antibiot 64, 117–122 (2011).
40. Todorovski T, Fedorova M, Hennig L & Hoffmann R Synthesis of peptides containing 5-hydroxytryptophan, oxindolylalanine, N-formylkynurenine and kynurenine. J. Pept. Sci 17, 256–262 (2011). [PubMed: 21254311]
41. Fuson RC The principle of vinylogy. Chem. Rev 16, 1–27 (1935).
42. Jhulki I, Chanani PK, Abdelwahed SH & Begley TP A remarkable oxidative cascade that replaces the riboflavin C8 methyl with an amino group during roseoflavin biosynthesis. J. Am. Chem. Soc 138, 8324–8327 (2016). [PubMed: 27331868]
43. Schwarz J, Konjik V, Jankowitsch F, Sandhoff R & Mack M Identification of the key enzyme of roseoflavin biosynthesis. Angew. Chem. Int. Ed 55, 6103–6106 (2016).
44. Konjik V et al. The crystal structure of RosB: insights into the reaction mechanism of the first member of a family of flavodoxin-like enzymes. Angew. Chem. Int. Ed 56, 1146–1151 (2017).
45. Kapoor I & Nair SK Structure-guided analyses of a key enzyme involved in the biosynthesis of an antivitamin. Biochemistry 57, 5282–5288 (2018). [PubMed: 30125480]
46. Ortega MA et al. Structure and tRNA specificity of MibB, a lantibiotic dehydratase from Actinobacteria involved in NAI-107 biosynthesis. Cell Chem. Biol 23, 370–380 (2016). [PubMed: 26877024]
47. Sherlin LD et al. Chemical and enzymatic synthesis of tRNAs for high-throughput crystallization. RNA 7, 1671–1678 (2001). [PubMed: 11720294]
48. Rio DC, Ares MJ, Hannon GJ & Nilsen TW RNA: a laboratory manual (Cold Spring Harbor Laboratory Press, 2011).
49. Walker SE & Fredrick K Preparation and evaluation of acylated tRNAs. Methods 44, 81–86 (2008). [PubMed: 18241790]

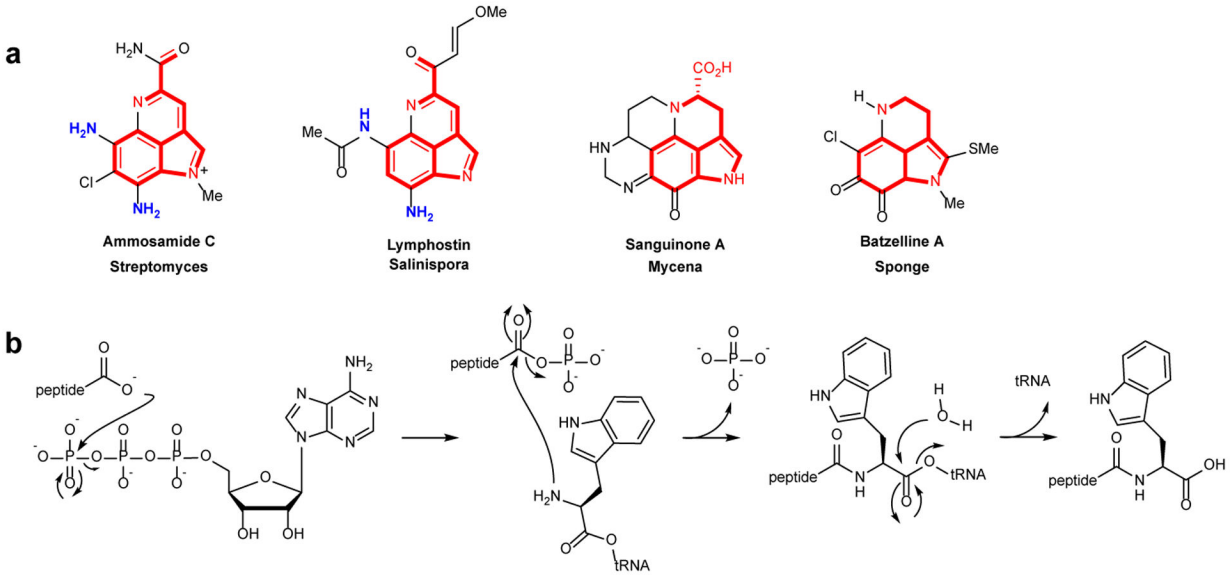

Fig. 1. Structures of pyrroloiminoquinone-derived natural products and activity of PEARL enzymes.

a, Representative examples of pyrroloiminoquinone-type natural products (also called pyrroloquinolines). The part of the structures shown in red highlight the atoms that likely derive from Trp. For family members for which the biosynthetic gene clusters are known, the current work shows that the amino groups depicted in blue likely originate from glycyl-tRNA and are installed by PEARLs. **b,** PEARL mechanism of non-ribosomal peptide extension during ammosamide biosynthesis.

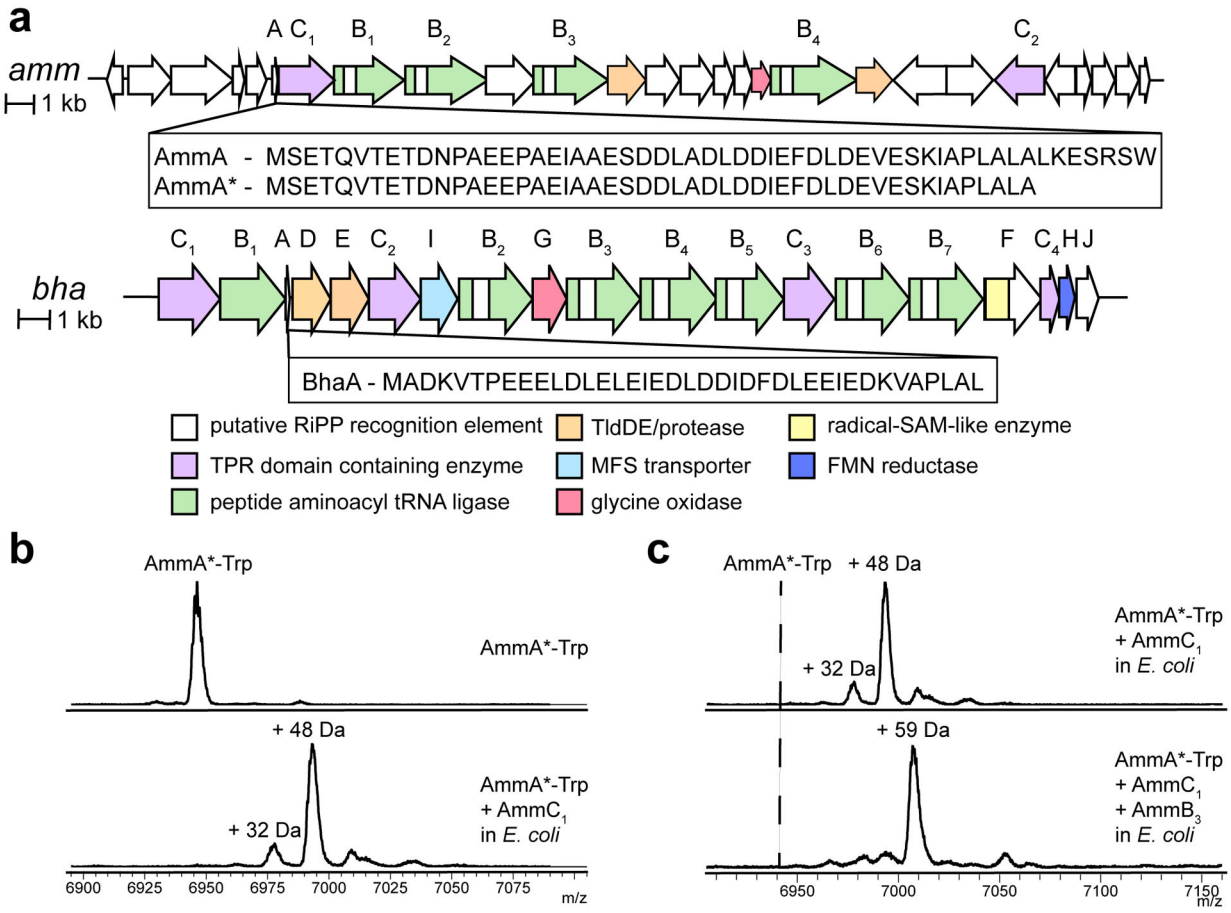

Fig. 2 |. Posttranslational modifications during ammosamide biosynthesis.

a, The *amm* and *bha* BGCs and the sequences of the precursor peptides. RRE encoding sequences are indicated as white bars in the gene. **b**, MALDI-TOF mass spectra of AmmA*-Trp (avg. mass calculated m/z 6941.1; observed 6941.8) and AmmA*-Trp co-expressed with $AmmC_1$ (avg. mass calculated m/z 6989.1; observed 6989.6). The two experiments were conducted side-by-side. **c**, MALDI-TOF mass spectrum of AmmA*-Trp co-expressed with $AmmC_1$ (avg mass calculated 6989.1; observed 6989.6) and AmmA*-Trp with $AmmC_1$ and $AmmB_3$ (avg. mass calculated m/z 7000.1; observed 7000.6). The co-expressions were conducted three times in independent experiments with similar results.

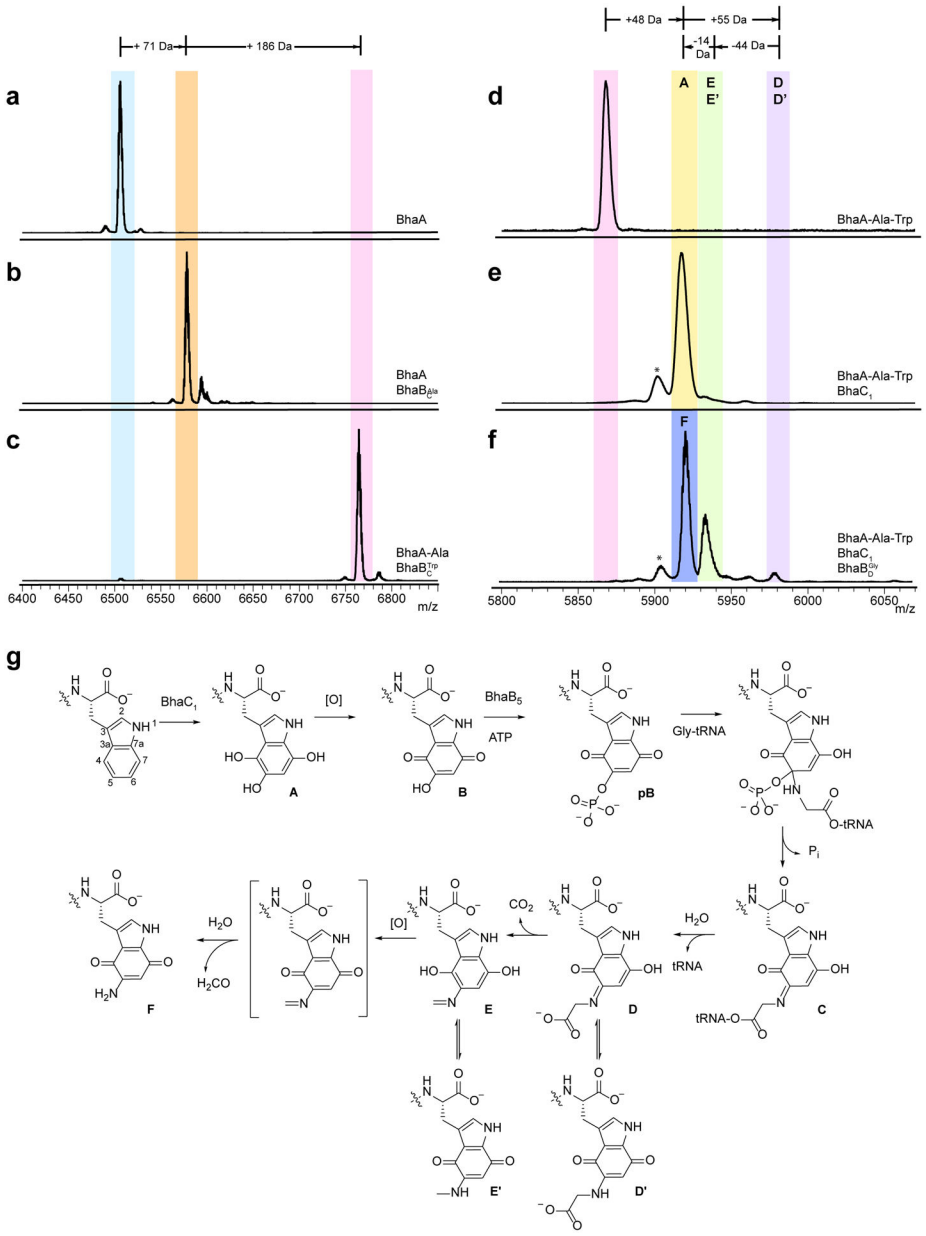

Fig. 3. Conversion of Trp to aminoquinone.

a-f, MALDI-TOF mass spectra of **a**, BhaA (calculated m/z 6502.1 Da; observed 6502.3 Da), **b**, BhaA co-expressed with BhaB$_1$ (renamed herein BhaB$_C^{Ala}$; calculated m/z 6573.1; observed 6573.2 Da), **c**, BhaA-Ala peptide co-expressed with BhaB$_7$ (renamed herein BhaB$_C^{Trp}$); calculated m/z 6759.2; observed 6760.5, **d**, BhaA-Ala-Trp (calculated m/z 5869.7; observed 5870.4), **e**, product from co-expression of BhaA-Ala-Trp with BhaC$_1$ (calculated m/z 5917.7; observed 5917.4), and **f**, products of co-expression of BhaA-Ala-Trp with BhaC$_1$ and BhaB$_5$ (renamed BhaB$_D^{Gly}$ herein); calculated m/z 5972.7; observed 5972.5. **g**, proposed mechanism of converting Trp to an aminoquinone. The co-expressions were repeated three times in independent experiments with similar results. The Bha-Ala-Trp

peptide in panel c was expressed from a different plasmid (pRSFDuet-1) than the peptide in panel d (pACYCDuet) accounting for their different masses. See coexpression section in Methods. The peaks labeled with * are deamination artifacts (M-17) from analysis by MALDI-TOF MS in positive reflector mode.

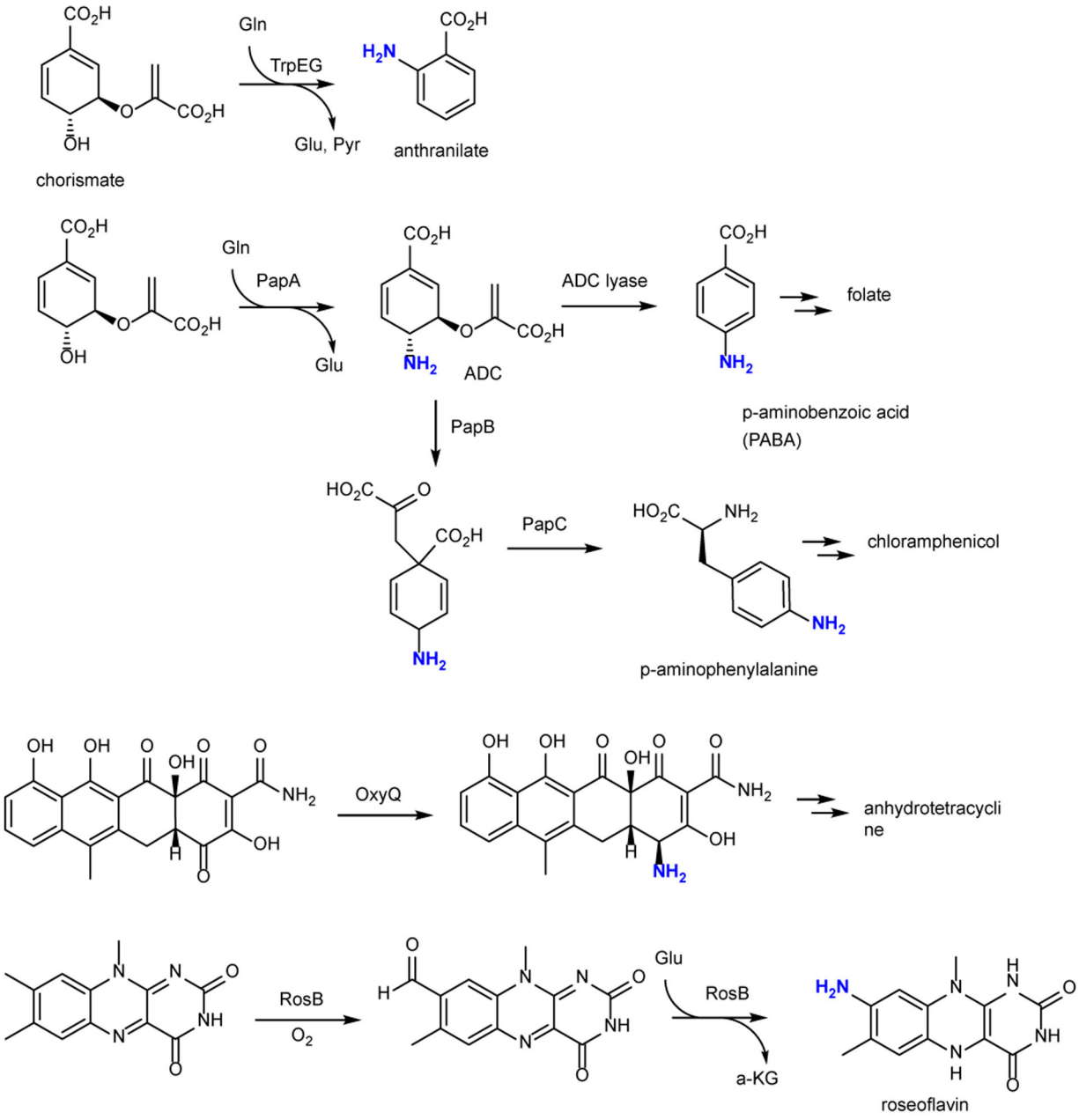

Fig. 4 |. Known pathways to aromatic amines.

Previously identified pathways to aromatic amines that typically involve Glu or Glu as the nitrogen donors.